Gold on carbon: influence of support properties on catalyst activity in liquid-phase oxidation

Claudia L. Bianchi [a], Serena Biella [b], Antonella Gervasini [a], Laura Prati [b,*], and Michele Rossi [b]

[a] Dipartimento di Chimica Fisica ed Elettrochimica, Università di Milano, via Golgi 19, 20133 Milano, Italy
[b] Dipartimento di Chimica Inorganica Metallorganica e Analitica e Centro CNR, Università di Milano, via Venezian 21, 20133 Milano, Italy

Received 28 May 2002; accepted 24 September 2002

Gold-on-carbon catalysts have been prepared from a preformed metallic phase (metal sol). Using, as the support, active carbons of different microstructure and surface properties, we found that each carbon affected differently the reactivity of the same gold particle in a standard liquid-phase oxidation, indicating that a specific metal–support interaction does exist, probably connected to the density of phenolic groups at the surface.

KEY WORDS: activated carbon; gold; oxidation catalyst; support effect.

1. Introduction

The importance of active carbon as a precious metal support in industrial chemistry is well recognized, carbons being stable in both acidic and basic media and being easily burnt off, a simple procedure for recovering the precious metal [1]. However, one major problem is that activated carbons are not manufactured specifically for catalysis, and it is difficult to obtain constant properties even from batch to batch of the same nominal material. The raw materials and the activation process are normally responsible for the surface microstructure and the chemical group distribution, whereas the presence of impurities like ashes and salts, which are potentially poisoning and/or pore plugging materials, depends on the washing treatment.

A typical application of carbon-supported metal is liquid-phase oxidation [2], and we recently reported the use of gold on carbon as a useful catalyst for the selective liquid-phase oxidation of glycols and aldehydes [3–6], although it has also been used in gas-phase processes like the hydrochlorination of ethyne [7] where gold has to be maintained as Au(III) to be active. In fact, the major problem is the tendency of the carbon itself to reduce the gold ions to the metallic state, as we have already noted during the preparation of Au(0) on carbon by deposition-precipitation [4].

The most useful method of providing good dispersion of gold metal on carbon has been shown to be the immobilization of the preformed metallic phase [8], although the choice of protecting agent for the metal particle is fundamental [5]. A second advantage of this method is the opportunity to modulate the mean diameter of the gold particle, and using this technique we were able to show that in the liquid-phase reaction of ethan-1,2-diol to glycolate, gold on carbon shows maximum activity when the mean diameter of the metal particle is around 7–8 nm [9].

We also highlighted that the anomalous behavior of carbon-supported gold, compared to other supports such as TiO_2, depends on a sort of shielding that the carbon itself makes on particles smaller than 7 nm that drop off in the matrix, the contact of the reagents being limited. However, using Au/C with a mean diameter of 7 nm gave us almost the same activity as using Au/TiO_2 with a mean gold particle diameter of 2–3 nm. Thus we hypothesize that carbon promotes the activity of the metal gold particle compared to oxidic supports. In order to highlight this effect we should deposit 2–3 nm sized particles on the external carbon surface or, alternatively, compare the behavior of metal particles of the same distribution on a series of different active carbons.

In this paper we used this second strategy using five activated carbons, characterized in terms of superficial area, porous structure and surface chemical composition.

2. Experimental

2.1. Materials

The powdered carbons used are listed in table 1. The pH was determined by suspending the carbon in distilled water and measuring after 1 h of equilibration time. Gold of 99.9999% purity in sponge, $NaBH_4$ of purity >96% from Fluka and polyvinylalcohol (PVA) ($M = 10\,000$) from Aldrich were used. Ethylene glycol was of the

* To whom correspondence should be addressed.
E-mail: Laura.Prati@unimi.it

1011-372X/03/0100-0091/0

Table 1
Summary of the carbons used

Supplier	Name	Origin	pH	Activation treatment	Washing
Carbosorb	MK	Wood	9–10	Physical activation	–
Camel	X40S	Coconut shell	8–9	Physical activation	–
Camel	Anthrafilter YV115	Coconut shell	9–10	Physical activation	–
Camel	Sorbpor ZV100E	Wood	4–7	Chemical activation	Water washed
Camel	Sorbpor X100S	Coconut shell	9–10	Physical activation	–

highest purity from Fluka and was used without any further purification. NaOH was 99.9% pure from Merck and stored under nitrogen. Gaseous oxygen from SIAD was 99.99% pure.

2.2. Carbon washing

The carbons were suspended in 6 M HCl and left under stirring for 12 h, then washed several times with distilled water by decantation until the pH of the solution reached values of 6–6.5. At the end the carbon was filtered off and dried for 5–6 h at 150 °C in air. The final water content was evaluated to be <3%.

2.3. Carbon characterization

Nitrogen (99.9995% purity) adsorption and desorption isotherms were obtained at liquid nitrogen temperature (−196 °C), using a Sorptomatic 1900 version instrument from Thermoquest that uses a static volumetric technique. The instrument was home-modified in order to measure the low-pressure values more accurately, by adding two pressure gauges working in the range 0–130 Pa and 0–13 kPa. The analysis was controlled by microcomputer processing using the MILES-200 program and the MILEADP program for computations. About 0.1 g of each sample was outgassed *in situ* for 16 h at 350 °C under a residual pressure of 1 Pa to remove moisture. The equilibrium pressure was determined as the point at which the pressure was stable to within 15 Pa for 5 min. Following this procedure, each adsorption lasted for ~20 h. The adsorbed volume, expressed in cm^3(STP)/g, was converted into pore volume, cm^3/g, using the density of N_2 in the normal liquid state ($\rho = 0.8081$ g/cm^3). The molecular area of N_2 was taken as 16.2 Å.

X-ray fluorescence was performed using a Jordan Valley EX-310 instrument equipped with a Rh anode at 35 kV reaching a maximum power of 9 W.

2.4. Carbon titrations

2.4.1. With $NaHCO_3$

A consistent amount of carbon (5 g) was weighed in a sealed flask to which 100 ml of a 0.1 M solution of $NaHCO_3$ were then added. After stirring the slurry for 16 h, the carbon was filtered off, washed several times with distilled water and the solution back-titrated using 0.2 M HCl. The result is expressed as consumed meq of $NaHCO_3$ per gram of carbon, corresponding to the presence of carboxylic groups on the surface.

2.4.2. With Na_2CO_3

A consistent amount of carbon (5 g) was weighed in a sealed flask to which 100 ml of a 0.1 M solution of Na_2CO_3 were then added. After stirring the slurry for 16 h, the carbon was filtered off, washed several times with distilled water and the solution back-titrated using 0.2 M HCl. The result is expressed as consumed meq of Na_2CO_3 − meq of $NaHCO_3$ per gram of carbon, corresponding to the presence of carboxylate, lactone groups on the surface.

2.4.3. With NaOH

A consistent amount of carbon (5 g) was weighed in a flask to which 100 ml of a 0.1 M solution of NaOH was then added. The slurry was thermostatted at 70 °C with a water bath for 8 h, this time being a suitable period for equilibration as reported in the literature [10]. After cooling at room temperature, the carbon was filtered off, washed several times with distilled water and the solution back-titrated using 0.2 M HCl. The result is expressed as consumed meq of NaOH − meq of Na_2CO_3 per gram of carbon, corresponding to the presence of phenolic groups on the surface.

2.5. Catalyst preparation

An aqueous $HAuCl_4$ solution of 100 μg/ml was prepared by dissolving gold (30 mg) in a minimum amount of HCl/HNO_3 (3/1 v/v) mixture and, after removing the HNO_3, diluting it with distilled water. Maintaining the auric solution under vigorous stirring, the 2 wt% PVA solution (0.96 ml) was added. A 0.1 M freshly prepared solution of $NaBH_4$ (7.62 ml) was then added dropwise, to yield to a ruby red metallic sol.

After a few minutes this was immobilized on carbon by adding the support under vigorous stirring. The amount of support was calculated as having a final gold loading of 1 wt%. After 1 h the slurry was filtered and the absorption of gold was checked by ICP analysis of the filtrate.

Before use, the catalysts were washed thoroughly with distilled water and then used in the wet form. The water content was determined by drying a sample for 5 h at 150 °C in air.

X-ray diffraction (XRD) experiments were performed using a Rigaku D III-MAX horizontal-scan powder diffractometer with CuKα radiation, equipped with a graphite monochromator in the diffracted beam. The crystallite sizes of the gold were estimated from peak half-widths by using Scherrer's equation with corrections for instrumental line broadening.

X-ray photoelectron spectroscopy (XPS) measurements were performed using an M-Probe instrument (SSI) equipped with a monochromatic AlKα source (1486.6 eV) with a spot size of 200 × 750 μm and a pass energy of 25 eV, providing a resolution of 0.74 eV.

The accuracy of the binding energies (BE) was estimated to be ±0.2 eV. All the samples were in this range around the value for metallic gold (84.0 eV). The quantitative data were checked accurately and reproduced several times (at least 10 times for each sample).

2.6. Catalytic test

The reactions were carried out in a thermostatted glass reactor (30 ml) provided with an electronically controlled magnetic stirrer connected to a large reservoir (5000 ml) containing oxygen at 300 kPa. The oxygen uptake was followed by a mass flow controller connected to a PC through an A/D board, plotting a flow/time diagram.

Ethylene glycol (8 mmol), NaOH (8.25 mmol) and the Au/C catalyst (glycol/metal = 1000 mol/mol) were mixed in distilled water (total volume 10 ml). The reactor was pressurized at 300 kPa of O_2 and thermostatted at 70 °C. After an equilibration time of 15 min, the mixture was stirred for 30 min and the products analyzed by HPLC using a Varian 9010 instrument equipped with a Varian 9050 UV (210 nm) and a Waters RI detector in series. An Alltech OA-1000 column (300 mm × 6.5 mm) was used with aqueous 0.01 M $H_{1s}O_4$ (pH 2.1) (0.8 ml/min) as the eluent. Samples of the reaction mixture (0.1 ml) were diluted (10 ml) using the eluent after adding the internal standard (propionic acid).

3. Results and discussion

Carbon properties as outlined in the introduction arise from the raw material itself and the activation process, and for their partial characterization we can use parameters like surface area, pore size distribution, surface chemical composition and checking for the presence of impurities.

Pore size distribution is important not only because it determines the surface area available but also because it controls the access of the substrate molecule to the supported metallic particles, access depending on particle allocation [9,11].

The oxygenated functionalities on the carbon surface (carboxylic groups, phenolic groups, lactones, quinones) are responsible for both the acid/base and redox properties of activated carbon. They also act as nucleation centers for metallic crystallites to be deposited on carbons [11–13].

Lastly, consideration must be given to the presence of inorganic impurities like calcium, potassium, iron and other heavy metals as these can change the acid/base or redox properties of the activated carbon. Moreover, ashes can vary the pH and micropore accessibility and also lead to a non-homogeneous distribution of the metallic phase on the support. It was for this reason that we pretreated the carbons with acidic washing and checked for inorganic impurity removal by fluorescence (table 2).

3.1. Characterization of carbons

3.1.1. Microstructure

The textural properties of the carbons determined from N_2 adsorption and desorption isotherms are reported in table 3 [14–16]. Surface areas were calculated by the *t-plot* method. The carbons derived from coconut shell all have surface areas around 1150–1250 m^2/g, while those derived from wood have a very different surface extent, about 1000 and 1700 m^2/g for MK and ZV100E, respectively. ZV100E has a ratio between the external and internal surface area completely different from the other samples. The external area (or interparticle void)

Table 2
Elements detected by fluorescence before washing[a]

Carbon			Element		
Raw material	Label	Activation	K	Ca	Fe
Coconut shell	X40S	Physical	Present	Present	Present
	X100S	Physical	Present	Present	Present
	YV115	Physical	Present	Present	Trace
Wood	MK	Physical	Present	Present	Trace
	ZV100E	Chemical	–	Trace	–

[a] 6 M HCl for 12 h followed by distilled water until the pH of the solution reached 6–6.5.

Table 3
Textural properties of carbons

Raw material	Carbon	Surface area (m^2/g)	Micropore volume [a] (cm^3/g)	E [a] (kJ/mol)	Pore diameter [b] (nm)
Coconut shell	X40S	1238	0.454	5.48	0.7–0.9
	X100S	1242	0.453	6.08	0.75–0.85
	YV115	1272	0.448	7.21	0.5–0.7
Wood	MK	1051	0.397	5.51	0.6–0.8
	ZV100E	1718	0.611	4.52	0.5–1.0

[a] Calculated according to Dubinin–Radushkevich equation.
[b] Calculated according to Horvath–Kawazoe equation.

is more than 30% of the total surface for ZV100E and around 5–6% of the total surface for all the other carbons.

The Dubinin–Radushkevich approach was applied to calculate the micropore volume and adsorption energy parameters of all the carbon samples. The coconut-derived carbons were found to have similar micropore volume values ($\sim$0.45 cm^3/g), while the adsorption energy (E, kJ/mol) varied significantly, the chemical composition and functional groups governing the interaction energy between N_2 and the pore walls. In contrast, the wood-derived carbons have very different micropore volumes: 0.611 and 0.397 cm^3/g for ZV100E and MK, respectively. ZV100E differed from MK also in the lower value of E (4.52 kJ/mol), which is the lowest among those calculated for all the other carbons.

3.1.2. Chemical surface composition

We limited our investigation to acidic groups as they have been studied in greater detail than basic ones [10,17]. Obviously, the present chemical characterization provides only an indication of the possible differences among the five activated carbons considered.

Adapting the Boehm procedure [18] we quantitatively determined the presence of free carboxylic acid (by $NaHCO_3$ titration), lactones, anhydrides (by titration with Na_2CO_3) and, finally, phenolic groups (by NaOH titration). In order to have consistent results the experimental procedure must be carried out very carefully, using a prolonged contact period to ensure equilibrium is reached. Table 4 shows the results, the carbons being presented in relation to the raw material from which they derive. The presence of carboxylic acids on the surface is almost the same in every case except for the case of ZV100E, the only carbon activated via a chemical process. This latter result is not surprising as chemical activation normally involves the use of a strong Lewis acid that, in principle, can hydrolyze lactones and anydrides, transforming them into carboxylic acid. In fact considering the sum of groups titrated with $NaHCO_3$ and Na_2CO_3 (corresponding to total Na_2CO_3 (meq/g) consumed) we observed that the ZV100E did not differ substantially from the others. In this case the exception is YV115 that presented a value (1.22 meq/g) about twice that of the mean value of the other carbons (0.58 meq/g).

A more evident difference among the carbons can be seen on considering the phenolic groups: once again YV115 presents the highest value (1.00 meq/g), followed by ZV100E (0.70 meq/g). The lowest value was calculated for X100S (0.28 meq/g).

3.2. Catalyst preparation and characterization

We have already reported on the preparation of a gold-on-carbon catalyst via immobilization of a metallic

Table 4
Results of basic titration (acid groups)

Carbon			Group [a]				
Raw material	Label	Activation	COOH (meq/g)	COOC (meq/g)	$\sum$ [b]	ArOH (meq/g)	$\sum$ [c]
Coconut shell	X40S	Physical	0.25	0.35	0.60	0.48	1.08
	X100S	Physical	0.28	0.32	0.60	0.28	0.88
	YV115	Physical	0.20	1.01	1.22	1.00	2.22
Wood	MK	Physical	0.24	0.28	0.52	0.52	1.04
	ZV100E	Chemical	0.60	–	0.60	0.70	1.30

[a] For experimental details see section 2.
[b] Sum of COOH and COOC groups corresponding to total meq/g of Na_2CO_3 consumed.
[c] Sum of COOH, COOC and ArOH groups corresponding to total meq/g of NaOH consumed.

Table 5
Gold-on-carbon catalyst characterization

Carbon	Au (%) [ICP]	Au(4f)/C(1s) (at%) [XPS]	*d* (nm) [XRPD]
X40S	1.00	1.34	10.85
X100S	0.90	1.62	11.65
YV115	0.82	0.29	11.80
MK	1.00	1.00	13.00
ZV100E	1.00	0.79	11.71

sol [5,8,9]. In principle, the method allows the deposition of almost the same sized gold particles on different carbons even though the carbons themselves, despite their similar microstructure, have a different chemical composition which could vary the metallic particle allocation. We have already demonstrated that the important parameters for gold-on-carbon activity in the liquid-phase oxidation of glycols are the dimensions of the gold particles and the degree of their exposure. Thus our first step in the present work was to characterize the catalyst obtained by XRPD (X-ray powder diffraction) and XPS (X-ray photoelectron spectroscopy) [9]. XRPD revealed (table 5) that the different nature of the activated carbons does not greatly affect the mean dimension of supported gold particles, and thus we were able to obtain supported gold particles with almost the same mean diameter, a prerequisite for correctly comparing XPS and catalytic data. The XPS data (table 5) show different atomic percentages Au(4f)/C(1s). This means that the different carbons shield the gold particles differently; the lowest value (0.29 at%) corresponds to YV115, the highest (1.62 at%) to X100S. However, we also had to consider that different carbon adsorption properties lead to different gold loadings (1–0.82%) which can also modify the value of Au(4f)/C(1s). Nevertheless, an approximate evaluation of the XPS data allows the highlighting of a correlation between Au(4f)/C(1s) and the presence of phenolic groups, the correlation with the phenolic groups being more evident than with the stronger acid carboxylic groups (figure 1). The general trend appeared to be that the greater the presence of the phenolic groups the greater the decrease in Au(4f)/C(1s).

3.3. Catalytic test

We noted that in the liquid-phase oxidation of ethylene glycol, the gold-on-carbon catalyst reaches maximum activity for a metal particle diameter centered around 7 nm, activity that largely depends on the exposure of gold [9]. In the same reaction we tested five Au/C differing in carbon support, our aim being to outline the role of the nature of the activated carbon on gold catalysis. Table 6 gives the catalytic results obtained in the oxidation of ethylene glycol at 343 K under a constant 300 kPa oxygen pressure. We have already demonstrated that the reactivity of gold on carbon in this reaction results from two summed factors: one intrinsic to the gold particle, the other relative to its accessibility [9]; now, we aim to demonstrate that also the intrinsic reactivity of the gold particle depends on the nature of the carbon, i.e. that there exists a support interaction mediating the reactivity. From TOFs (turn-over frequencies) calculated on total gold loading (table 6) we observed that particles of almost the same mean dimension (11–13 nm) resulted in different reactivity, depending on the carbon used as the support. The most active appeared to be gold on YV115, but this result appeared surprising considering that this catalyst shows the lowest fraction of gold on the external surface (Au(4f)/C(1s) = 0.29 at%).

It seems that the greater the depth of the gold particles under the surface, the more the activity increases. This could indicate that when gold particles are located more deeply there should be greater interaction with

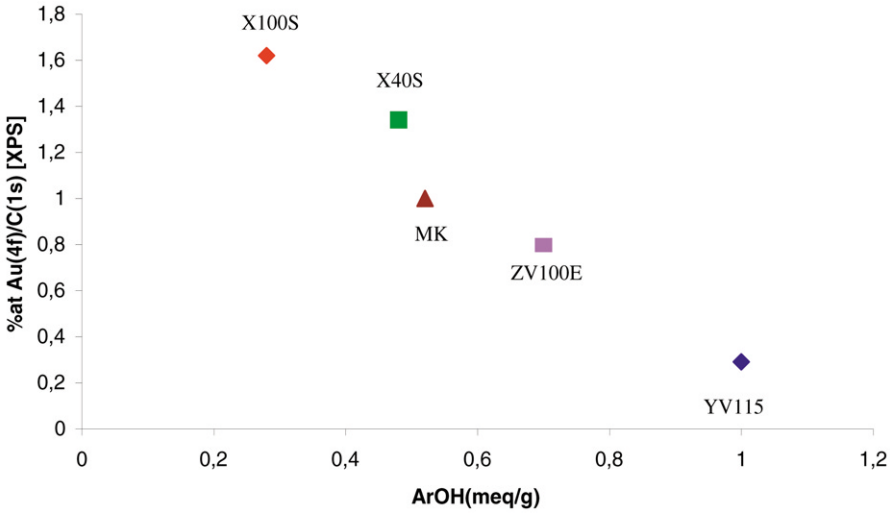

Figure 1. Correlation between atomic percentage of Au(4f)/C(1s) determined by XPS and phenolic groups.

Table 6
Catalytic results [a]

Catalyst	Au(4f)/C(1s) (at%)	TOF (per h) [b]
1% Au/X40S	1.34	970
0.9% Au/X100S	1.62	830
0.82% Au/YV115	0.29	1290
1% Au/MK	1.00	895
1% Au/ZV100E	0.79	950

[a] Catalytic test: ethylene glycol (8 mmol); NaOH (8.25 mmol); Au/C catalyst (glycol/metal = 1000 mol/mol); distilled water (total volume 10 ml); $pO_2 = 300$ kPa; $T = 343$ K; $t = 1$ h.
[b] Based on total gold.

Table 7
Correlation between catalytic activity and surface properties of carbons

	YV115	ZV100E	MK	X40S	X100S
ArOH [a] (meq/g)	1.00	0.70	0.52	0.48	0.28
Au(4f)/C(1s) (at%) [XPS]	0.29	0.79	1.00	1.34	1.62
TOF (per h) [b]	1290	950	895	970	830

[a] Determined by titration with NaOH (see section 2).
[b] Based on total gold.

the carbon (table 7). This conclusion is also supported by the energy interaction (E in table 3) with N_2, that is a maximum for YV115.

4. Conclusion

Through the screening of a gold catalyst supported on different activated carbons we have gained insight into gold reactivity in liquid-phase oxidation.

First we highlighted a correlation between the presence of phenolic groups and the atomic percentage of exposed gold (Au(4f)/C(1s)), a correlation observed to correspond with increasing catalyst activity (table 7). Conversely, gold particle exposure is not directly connected with microstructure as all the carbons were similar with regard to microporous nature; thus it could be that it is the surface chemical composition that induces the higher shielding of gold particles as evidenced by XPS.

The most active catalyst was gold supported on the YV115 coconut shell-derived carbon. This catalyst showed the highest TOF even though it had the lowest atomic percentage of exposed gold, meaning that the YV115 carbon promoted the gold particle activity in a surprising manner, so much so in fact that this promotion dominates the effect of the minor surface exposure that we had already demonstrated to be a limiting gold reactivity factor in the liquid phase [9].

Further investigations into the true nature of the activated carbon surface could provide a greater understanding of the factors affecting the catalytic activity of gold particles. However, for the moment titration with NaOH appears a good tool for screening carbons able to enhance gold activity in liquid-phase oxidation applications.

Acknowledgments

Camel Chemicals S.p.A. is gratefully acknowledged for its generous carbon supplies.

References

[1] E. Auer, A. Freund, J. Pietsch and T. Tacke, Appl. Catal. A: Gen. 173 (1998) 259.
[2] T. Mallat and A. Baiker, Catal. Today 19 (1994) 247.
[3] L. Prati and M. Rossi, Stud. Surf. Sci. Catal. 110 (1997) 509.
[4] L. Prati and M. Rossi, J. Catal. 176 (1998) 552.
[5] S. Coluccia, G. Martra, F. Porta, L. Prati and M. Rossi, Catal. Today 61 (2000) 165.
[6] S. Biella, L. Prati and M. Rossi, J. Catal. 206 (2002) 242.
[7] G.J. Hutchings, Gold Bull. 29 (1996) 123, and references therein.
[8] L. Prati and G. Martra, Gold Bull. 32 (1999) 96.
[9] C. Bianchi, F. Porta, L. Prati and M. Rossi, Topics Catal. 13 (2000) 231.
[10] H.-P. Boehm, Adv. Catal. 13 (1962) 137.
[11] D.S. Cameron, S.J. Cooper, I.L. Dodgson, B. Harrison and J.W. Jenkins, Catal. Today 7 (1990) 113.
[12] M.A. Corapcioglu and C.P. Huang, Carbon 25 (1987) 569.
[13] C.A. Leon, Y. Leon, J.M. Solar, V. Calemma and L.R. Radovic, Carbon 30 (1992) 797.
[14] S. Brunauer, L.S. Deming, W.E. Deming and E. Teller, J. Am. Chem. Soc. 62 (1940) 1723.
[15] G. Horvath and K. Kawazoe, J. Chem. Eng. Jpn. 16 (1983) 470.
[16] H.Y. Zhu, N. Maes, A. Molinard and E.F. Vansant, Microporous Mater. 3 (1994) 235.
[17] C. Ishizaki and I. Marti, Carbon 19 (1981) 409.
[18] H.-P. Boehm, E. Diehl, W. Heck and R. Sappok, Angew. Chem. Int. Ed. 3 (1964) 669.